Nanostructures

DOI: 10.1002/ange.200601553

Crystalline Nanoflowers with Different Chemical Compositions and Physical Properties Grown by Limited Ligand Protection**

*Arun Narayanaswamy, Huifang Xu, Narayan Pradhan, and Xiaogang Peng**

Colloidal nanocrystals with controlled size and shape play a key role in nanotechnology.[1–3] Organometallic[4–6] and related alternative (or so-called greener)[7–10] synthetic methods at elevated temperatures in non-aqueous solvents are the current mainstream strategies for producing high-quality nanocrystals. The ability to control the size and size distribution of nanodots using these strategies is reasonably well developed. Also, advances in the formation of 1D nanocrystals have recently been reported.[5,11–14] These 1D structures offer a unique technical potential that is inaccessible with the corresponding 0D nanocrystals. Reports on the synthesis of complex 3D nanostructures, however, remain uncommon.[15–19] Most of these structures are grown on substrates, are large in size, and/or are polycrystalline. Herein, we demonstrate that, by simply reducing the degree of ligand protection to the domain of limited ligand protection (LLP), the existing mainstream synthetic chemistry for 0D and 1D nanocrystals—more specifically, the greener approaches—can also produce high-quality complex 3D nanostructures, such as crystalline nanoflowers. Unlike the formation of tetrapods of II–VI semiconductors with specific crystal structures,[15,20] we reveal that LLP coupled with 3D oriented attachment can be applied in the preparation of nanocrystals with different compositions, crystal structures, and physical (magnetic and electronic) properties.

The LLP strategy was first applied to the In_2O_3 nanocrystal system, and it was not clear if the 3D oriented attachment caused by LLP would be limited to certain crystal structures and compositions. Herein, we intend to clarify the generality of the LLP strategy. A detailed account of the nanocrystal growth mechanism will be reported separately.[21]

A metal carboxylate (acetate (Ac), myristate (Mt), or stearate (St)) was used as a precursor, and a generic hydrocarbon, such as 1-octadecene (ODE), was used as solvent. Myristic acid (MA) or stearic acid (SA) was optionally used as a free ligand. An alcohol, such as 1-octadecyl alcohol (OA) or decyl alcohol (DA), was often added to either activate the stable precursors or to increase the yield and stability[22] of the oxide nanoflowers. For the ZnSe nanoflowers, an amine, such as 1-octadecyl amine (ODA), was used as an activation reagent and a ligand, and selenium powder dissolved in tributylphosphine was used as a reagent.

The results for the model system of In_2O_3 are briefly summarized in Figure 1, which shows representative transmission electron microscope (TEM) images of the nanostructures formed. When $In(Ac)_3$ is used as the precursor, the extremely short Ac ligands require that a high concentration (2 equiv) of MA be used to stabilize dot-shaped nanocrystals in the domain of sufficient ligand protection (SLP; Figure 1, center panel, top left). If only 1 equivalent of the long-chain fatty acid is present, the system is in the LLP domain. The individual nanodots become unstable and aggregate into 3D nanoflowers (Figure 1, center panel, top right). LLP can also be achieved with indium salts of fatty acids with long hydrocarbon chains, such as $In(Mt)_3$, without addition of free MA (Figure 1, center panel, bottom right). In comparison, the addition of 1 equiv of free MA yields nearly monodisperse nanodots (Figure 1, center panel, bottom left). All four reactions were carried out under the same conditions, with the exception of the types and concentrations of the indium precursors and ligands.

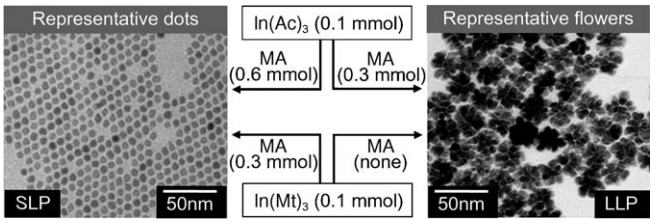

Figure 1. Formation of In_2O_3 nanodots by SLP and nanoflowers by LLP, and representative TEM images of the nanostructures (the size and shape depend on the reaction conditions).

Figure 2 illustrates that a variety of reaction systems can be similarly tuned to either the regular SLP domain or the LLP domain, through the use of metal carboxylates as precursors and the optional addition of a free ligand in a low concentration. This simple approach allows the growth of both nearly monodisperse nanoparticles and nanoflowers without any size sorting.

The size and shape of the 3D nanostructures can be varied in several different ways (Figure 3). The number of primary particles in each 3D ZnO aggregate is similar when MA (Figure 3a) or SA (Figure 3b) is used as the free ligand, but the sizes of the primary particles are different. When a lower concentration of the free fatty acid (MA) is used (Figure 3c), the number of primary particles in each ZnO nanoflower increases dramatically. The primary particles in the CoO nanoflowers formed in the early stages of the reaction (Figure 3e) are pointier and less regular in shape than those found in later stages (Figure 3f).

[*] Dr. A. Narayanaswamy, Dr. N. Pradhan, Dr. X. Peng
Department of Chemistry and Biochemistry
University of Arkansas
Fayetteville, AR 72701 (USA)
Fax: (+1) 479-575-4049
E-mail: xpeng@uark.edu
Dr. H. Xu
Department of Geology and Geophysics
University of Wisconsin
Madison, WI 53706 (USA)

[**] Financial support from the National Science Foundation (X.P.) and Wisconsin Alumni Research Foundation (H.X.) is acknowledged.

Supporting information for this article is available on the WWW under http://www.angewandte.org or from the author.

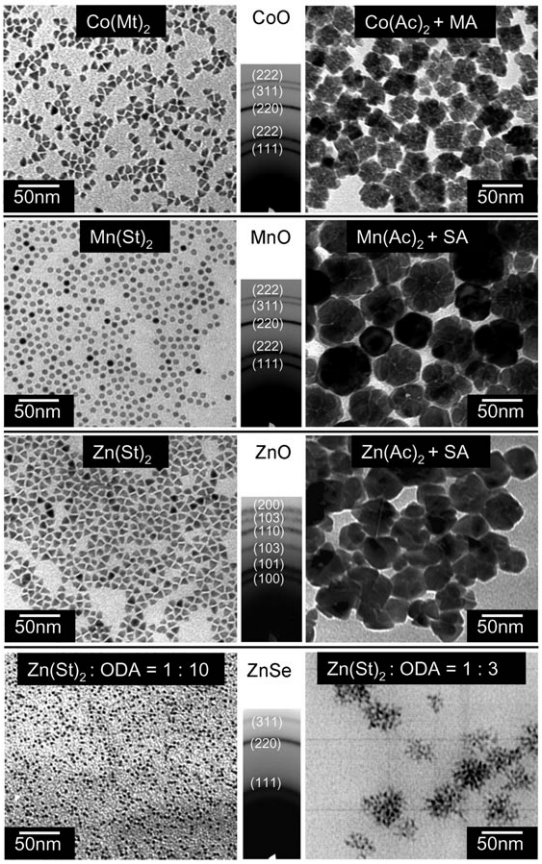

Figure 2. TEM images of the nanoparticles (left) and nanoflowers (right) formed in the CoO, MnO, ZnO, and ZnSe systems, and corresponding selected-area electron diffraction (SAED) patterns (center). The metal precursors and free ligands used in each system are indicated.

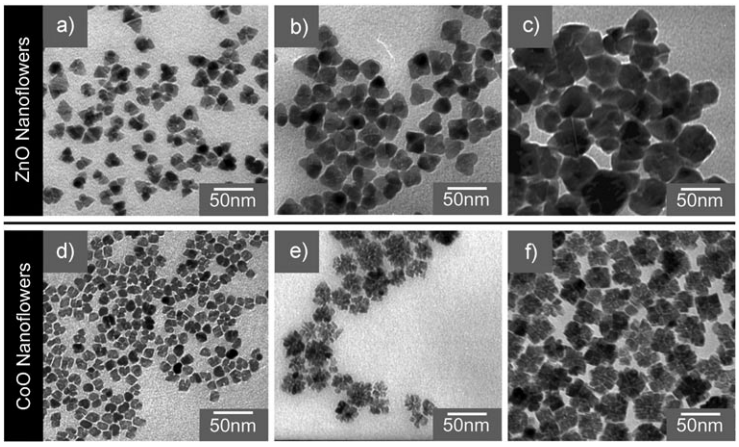

Figure 3. TEM images of the ZnO and CoO nanoflowers formed under different reaction conditions: a) $Zn(Ac)_2$:MA = 1:4, b) $Zn(Ac)_2$:SA = 1:4, c) $Zn(Ac)_2$:MA = 1:1, d) $Co(Ac)_2 \cdot 4H_2O$:MA = 1:2, e) $Co(Ac)_2 \cdot 4H_2O$:SA = 1:2, 5 min after addition of DA, f) $Co(Ac)_2 \cdot 4H_2O$:SA = 1:2, 20 min after addition of DA.

The five types of nanocrystals formed belong to four different crystal structures: bixbyite (cubic) for In_2O_3, rock salt (cubic) for CoO and MnO, wurtzite (hexagonal) for ZnO, and zinc blende (cubic) for ZnSe. The ZnO nanocrystals have an electric dipole moment in the direction of the unique *c* axis of the wurtzite structure. The CoO and MnO nanocrystals have a magnetic dipole. The ratio of cations to anions in In_2O_3 differs from that in the other compounds. Even for the same cation to anion ratio (1:1), the coordination number of the cation differs from case to case, being six in MnO and CoO, and four in ZnO and ZnSe. ZnO and ZnSe are well-known semiconductors.

Although LLP occurs in a variety of systems, there are some noticeable differences among the resulting nanoflowers (Figures 1–3). The primary nanocrystals in the In_2O_3 and ZnSe nanoflowers do not seem to be faceted. The MnO nanoflowers are formed by faceted primary particles, but the primary nanocrystals do not seem to have a fixed morphology. The ZnO nanoflowers are formed by nanopyramid primary particles (Figure 4). The primary nanocrystals in the CoO nanoflowers appear to be cubic. Evidently, the shapes of the primary nanocrystals constituting a nanoflower are not necessarily the same as those of the corresponding individual nanocrystals grown under SLP (Figure 2).

The oriented attachment of the primary nanocrystals to yield nanoflowers was studied by high-resolution (HR)TEM. Oriented attachment refers to the formation of relatively large crystalline structures by the attachment of crystalline primary particles, typically dot-shaped nanocrystals.[23] The 1D oriented attachment of nanodots to form nanorods or nanowires has been well documented, and there is strong evidence that an electric dipole moment is the major driving force.[12–14] Similarly, it has been reported that ferromagnetic nanodots can be self-assembled into 1D nanowires by magnetic dipole–dipole interactions between the primary particles in solution.[24]

Kotov and co-workers clearly demonstrated that, for the 1D oriented attachment of CdTe nanocrystals, it was essential to remove excess ligands in the reaction solution after the formation of the primary CdTe nanodots.[13] Although some reports have suggested that certain 3D nanostructures are formed through 3D oriented attachment in the nanometer regime,[25–27] the evidence is less convincing than in the 1D case. Controlled 3D oriented attachment on the nanoscale through the manipulation of ligand protection has not yet been reported.

HRTEM indicates that 3D oriented attachment occurs, either perfectly (In_2O_3 and CoO) or imperfectly (ZnO and MnO), in the formation of the nanoflowers. The results for the ZnO nanocrystals are particularly interesting. The primary particles of the ZnO nanoflowers are faceted, mainly with a pyramid shape (Figure 4). Stacking faults that may result in local zinc blende-like domains occur in some of the nanopyramids. The imperfection of the 3D oriented attachment[23] can be seen in this case: most of the ZnO nanocrystals attach to form a flower with a common crystallographic orientation, but a small misalignment is observed between some nanocrystals (for example, the 1.5° mismatch between the (100) lattice fringes in the left and right nanocrystals in the center panel of Figure 4). The ZnO nanocrystals attach to each other by sharing several different faces, including their $(00\bar{1})$ faces (Figure 4). Thus, the attachment cannot be caused by an electric-dipole mechanism. As discussed below, the attach-

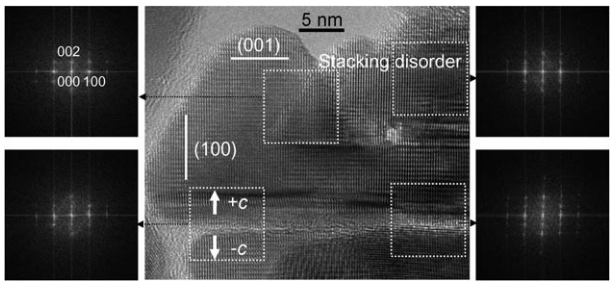

Figure 4. HRTEM image of part of a ZnO nanoflower (center), and fast Fourier transforms (FFTs; left and right) of selected areas (dotted squares) of the HRTEM image. See text for details.

ment of the $(00\bar{1})$ face of one primary nanocrystal to the (001) face of the next to form 1D ZnO nanowires would be expected if the electric dipole, in the direction of the unique *c* axis of the wurtzite structure, were playing a determining role.

Weller and co-workers convincingly showed that ZnO nanorods could be formed by the 1D oriented attachment of spherical nanodots along their *c* axis in an alcohol solution.[12] However, although ZnO nanocrystals have a dipole moment along their *c* axis, 3D oriented attachment can still occur, as shown in Figure 4. In comparison to our experimental conditions, Weller and co-workers used shorter ligands (Ac as the sole ligand) and a significantly lower temperature (60 °C). The very short ligands greatly decreased the distance between primary particles and, thereby, enhanced the dipole interaction between them. The low reaction temperature reduced the thermal energy of the primary particles, allowing them to align their dipole moments during the attachment events.

Significantly more experiments are needed to clarify this interesting system. The attachment of primary particles in one, two, or three dimensions in a controllable fashion is of considerable appeal. Further insight into this system may also help us to understand natural mineralization processes occurring under high-temperature and high-pressure conditions. In these processes, 3D attachment, either perfect or imperfect, should be preferred.

Similar to the electric dipole, the magnetic dipole does not play a determining role in the 3D oriented attachment of the magnetic CoO and MnO nanocrystals. Furthermore, both the CoO and MnO nanoflowers are crystalline in nature, but the MnO nanoflowers show some signs of imperfect oriented attachment (a detailed structural analysis will be published separately).

Although LLP makes individual nanodots unstable, the resulting nanoflowers are generally stable in the reaction solution and are also dispersible in nonpolar solvents after purification. The stability of the nanoflowers is probably a result of their complex surface structure. The ligands bound to surface atoms in the gaps between incompletely fused primary nanocrystals are kinetically "trapped" and, hence, difficult to remove. Similarly, tetrapods and highly branched nanocrystals of CdSe and CdTe were found to be more durable and dispersible than the corresponding nanorods.[15,20,28]

In summary, a unique and general approach, LLP, has been developed for the growth of nearly monodisperse nanostructures through 3D oriented attachment. With LLP, the primary nanocrystals are insufficiently protected, but the resulting 3D nanostructures are stabilized. This principle implies that LLP may be applicable to a broad spectrum of colloidal nanocrystals, without drastically altering the synthetic chemistry established for 0D and 1D nanocrystals in the recent years. Our results indicate that oriented attachment, at least in the 3D case, does not need to be driven by an electric or magnetic dipole moment. A detailed analysis of this issue for the In_2O_3 model system will be published shortly.[21] The complex crystalline nanostructures described herein offer unique nanoarchitectures for the development of high-performance electronic, optoelectronic, and sensing devices. The discovery of the LLP domain in the mainstream synthetic chemistry of high-quality nanocrystals enhances this important materials field. Although 1D oriented attachment has been well documented, the results herein indicate that 3D oriented attachment with LLP may occur more generally in natural mineralization and materials synthesis, especially under relatively vigorous conditions.

Experimental Section

Individual nanocrystals (dots or pyramids) of In_2O_3, ZnO, CoO, and MnO were produced by injecting the corresponding metal salt of a long-chain fatty acid (MA or SA) into a mixture of OA and ODE at 290 °C. In a typical synthesis of ZnO nanocrystals, $Zn(St)_2$ (0.1 mmol) and ODE (4 g) were loaded into a 25-mL three-necked flask, degassed, and heated to 280 °C under an argon atmosphere. OA (0.5 mmol) dissolved in ODE (0.5 g) at 150 °C was then injected into the mixture, and the temperature was decreased to 250 °C. After incubating for 10 min at 250 °C, SA (0.1 mmol) dissolved in ODE (0.5 g) at 120 °C was injected into the reaction mixture. The resulting mixture was incubated for 1 h to yield pyramid-shaped ZnO nanocrystals.

Nanoflowers of In_2O_3, ZnO, CoO, and MnO were formed from the corresponding metal acetates in the presence of MA or SA. In a typical synthesis of ZnO nanoflowers, anhydrous $Zn(Ac)_2$ (0.1 mmol), SA or MA (0.1 mmol), and ODE (4.75 g) were heated to 280 °C under an argon atmosphere. DA (0.75 mmol) in ODE (0.5 g) was then injected into the mixture to yield ZnO nanoflowers. Details of the syntheses of individual nanocrystals and nanoflowers of In_2O_3, CoO, MnO, and ZnSe are given in the Supporting Information.

Received: April 19, 2006
Published online: July 6, 2006

Keywords: crystal growth · ligand protection · nanostructures · oriented attachment · oxides

[1] C. B. Murray, C. R. Kagan, M. G. Bawendi, *Annu. Rev. Mater. Sci.* **2000**, *30*, 545.
[2] M. Yin, C.-K. Wu, Y. Lou, C. Burda, J. T. Koberstein, Y. Zhu, S. O'Brien, *J. Am. Chem. Soc.* **2005**, *127*, 9506.
[3] X. Peng, J. Thessing, *Struct. Bonding (Berlin)* **2005**, *118*, 79.
[4] C. B. Murray, D. J. Norris, M. G. Bawendi, *J. Am. Chem. Soc.* **1993**, *115*, 8706.
[5] X. Peng, U. Manna, W. Yang, J. Wickham, E. Scher, A. Kadavanich, A. P. Alivisatos, *Nature* **2000**, *404*, 59.

[6] T. Hyeon, S. S. Lee, J. Park, Y. Chung, H. B. Na, *J. Am. Chem. Soc.* **2001**, *123*, 12798.
[7] Z. A. Peng, X. Peng, *J. Am. Chem. Soc.* **2001**, *123*, 183.
[8] W. W. Yu, X. Peng, *Angew. Chem.* **2002**, *114*, 2474; *Angew. Chem. Int. Ed.* **2002**, *41*, 2368.
[9] S. Sun, H. Zeng, *J. Am. Chem. Soc.* **2002**, *124*, 8204.
[10] N. R. Jana, Y. Chen, X. Peng, *Chem. Mater.* **2004**, *16*, 3931.
[11] T. J. Trentler, K. M. Hickman, S. C. Goel, A. M. Viano, P. C. Gibbons, W. E. Buhro, *Science* **1995**, *270*, 1791.
[12] C. Pacholski, A. Kornowski, H. Weller, *Angew. Chem.* **2002**, *114*, 1234; *Angew. Chem. Int. Ed.* **2002**, *41*, 1188.
[13] Z. Tang, N. A. Kotov, M. Giersig, *Science* **2002**, *297*, 237.
[14] K.-S. Cho, D. V. Talapin, W. Gaschler, C. B. Murray, *J. Am. Chem. Soc.* **2005**, *127*, 7140.
[15] L. Manna, D. J. Milliron, A. Meisel, E. C. Scher, A. P. Alivisatos, *Nat. Mater.* **2003**, *2*, 382.
[16] Z. R. Tian, J. A. Voigt, J. Liu, B. McKenzie, M. J. McDermott, M. A. Rodriguez, H. Konishi, H. Xu, *Nat. Mater.* **2003**, *2*, 821.
[17] B. Liu, H. C. Zeng, *J. Am. Chem. Soc.* **2004**, *126*, 8124.
[18] Z. Zhang, H. Sun, X. Shao, D. Li, H. Yu, M. Han, *Adv. Mater.* **2005**, *17*, 42.
[19] J. Chen, T. Herricks, Y. Xia, *Angew. Chem.* **2005**, *117*, 2645; *Angew. Chem. Int. Ed.* **2005**, *44*, 2589.
[20] W. W. Yu, Y. A. Wang, X. Peng, *Chem. Mater.* **2003**, *15*, 4300.
[21] A. Narayanaswamy, H. Xu, N. Pradhan, X. Peng, *J. Am. Chem. Soc.*, in press.
[22] Y. Chen, M. Kim, G. Lian, M. B. Johnson, X. Peng, *J. Am. Chem. Soc.* **2005**, *127*, 13331.
[23] R. L. Penn, J. F. Banfield, *Science* **1998**, *281*, 969.
[24] J. Gao, B. Zhang, X. Zhang, B. Xu, *Angew. Chem.* **2006**, *118*, 1242; *Angew. Chem. Int. Ed.* **2006**, *45*, 1220.
[25] H. G. Yang, H. C. Zeng, *Angew. Chem.* **2004**, *116*, 6056; *Angew. Chem. Int. Ed.* **2004**, *43*, 5930.
[26] D. Zitoun, N. Pinna, N. Frolet, C. Belin, *J. Am. Chem. Soc.* **2005**, *127*, 15034.
[27] V. Tzitzios, D. Niarchos, M. Gjoka, N. Boukos, D. Petridis, *J. Am. Chem. Soc.* **2005**, *127*, 13756.
[28] Z. A. Peng, X. Peng, *J. Am. Chem. Soc.* **2002**, *124*, 3343.

